

Two-fermion and Two-photon Final States at LEP2 and Search for Extra Dimensions

Dimitri Bourilkov*

Institute for Particle Physics (IPP), ETH Zürich,
CH-8093 Zürich, Switzerland

Invited LEP2 review talk
Les Rencontres de Physique de la Vallée d'Aoste
La Thuile, Aosta Valley, Italy, 4-10 March 2001

Abstract

For the first time the experiments ALEPH, DELPHI, L3 and OPAL have presented *preliminary* results for fermion-pair and photon-pair production in e^+e^- collisions on the full LEP2 data set. The details of the experimental measurements and results from their LEP-wide combination are presented. No statistically significant deviations from the Standard Model expectations are observed and lower limits, some obtained in dedicated analyses, for new physics phenomena at 95 % confidence level are derived. The scales of contact interactions are constrained to lie above 10–20 TeV, depending on the helicity structure. The Standard Model has thus been tested at LEP2 down to distances $10^{-19} - 10^{-20}$ m. This has many implications, one example being the interpretation of the new result on the anomalous magnetic moment of the muon as coming from muon sub-structure. For $\gamma\gamma$ final states the QED cut-offs are $\Lambda_+ > 0.44$ TeV and $\Lambda_- > 0.37$ TeV. In a combined analysis, using e^+e^- and $\gamma\gamma$ final states, the most stringent lower limits to date, $M_s^+ > 1.13$ TeV ($\lambda = +1$) and $M_s^- > 1.39$ TeV ($\lambda = -1$), on the low gravity effective Planck scale are set. Constrains on the scales of string models like *TeV strings* and *D-branes* are derived. In the last case the lower limit is 1.5 – 4 TeV, depending on the coupling strength.

*e-mail: Dimitri.Bourilkov@cern.ch, Web: <http://cern.ch/bourilkov/>

1 Introduction

Data

The four LEP collaborations ALEPH, DELPHI, L3 and OPAL have taken data at energies above the Z resonance from 1995, starting at 130 GeV, until November 2000, culminating at energies close to 209 GeV. For the first time we have results on the full LEP2 data set, giving a flavor of the expected final experimental precision and sensitivity to physics beyond the Standard Model (SM). With minor exceptions, the data up to 189 GeV centre-of-mass energy are final, and the data collected in 1999 and 2000 at energies between 192–209 GeV *preliminary*. The luminosity accumulated above the Z pole in a single experiment is summarized in Table 1.

Table 1: Data collected in a single experiment above the Z resonance.

Year	\sqrt{s} GeV	$\mathcal{L}/\text{exp.}$ pb^{-1}	$\sigma_{q\bar{q}}$ - stat. err. [%]/exp. total / HE	Mode of operation
1995 & 97	130	6	2.3/5.2	Above
1995 & 97	136	6	2.6/6.0	M_Z
1996	161	10	2.7/5.9	W pairs
1996	172	10	3.2/7.3	W mass
1997	183	55	1.4/3.3	Z pairs
1998	189	177	0.8/1.8	High
1999	192-202	233	0.7/1.6	precision
2000	202-209	220	0.7/1.6	Higgs
1995-2000	130-209	720	0.4/0.8	LEP2

In the same table the statistical error on the hadronic cross section is given in %. The combined error for the total sample is $\sim 0.4\%$, and for the most interesting non-radiative (or genuine high energy) sample $\sim 0.8\%$. If we combine the measurements of the four experiments the statistical error is reduced by a factor of two. Clearly LEP2 has reached the phase of high precision, putting additional requirements on the careful study of systematic effects and on matchingly accurate theory predictions.

Fermion-pair Production

In the Standard Model the production of a fermion-pair in e^+e^- collisions is described by the exchange of γ or Z in the s -channel, and if the final state is identical to the initial one, also in the t -channel (*cf.* Figure 1).

The differential cross section has the form:

$$\frac{d\sigma}{d\Omega} = |\gamma_s + Z_s + \text{elec} * (\gamma_t + Z_t) + \text{New Physics ?!}|^2 \quad (1)$$

where the contributing amplitudes are denoted symbolically by γ_s , Z_s , γ_t and Z_t .

As an illustration the hadron cross is given in Figure 2 as a function of the centre-of-mass energy. The contributions from photon or Z exchange are shown separately together with the total cross section, which includes also interference effects. We can observe that at 200 GeV the

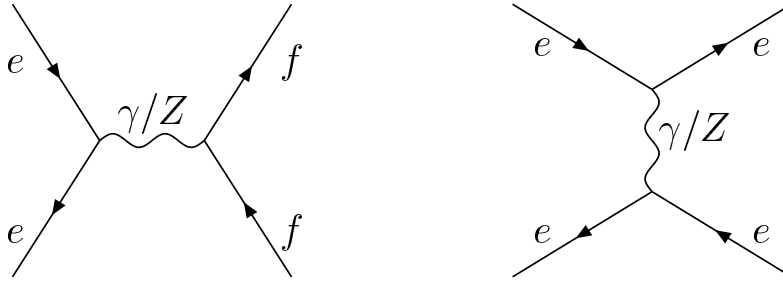


Figure 1: *Standard Model Feynman diagrams for difermion final states.*

contribution from photon exchange has a size similar to the one coming from Z exchange. For leptonic final states, due to the higher electric charges, the photon exchange dominates. In the same figure the forward-backward asymmetry for muons is shown. Here the contributions from photon or Z exchange show up as straight lines close to zero, and the large positive asymmetry above the Z pole is totally dominated by the interference term.

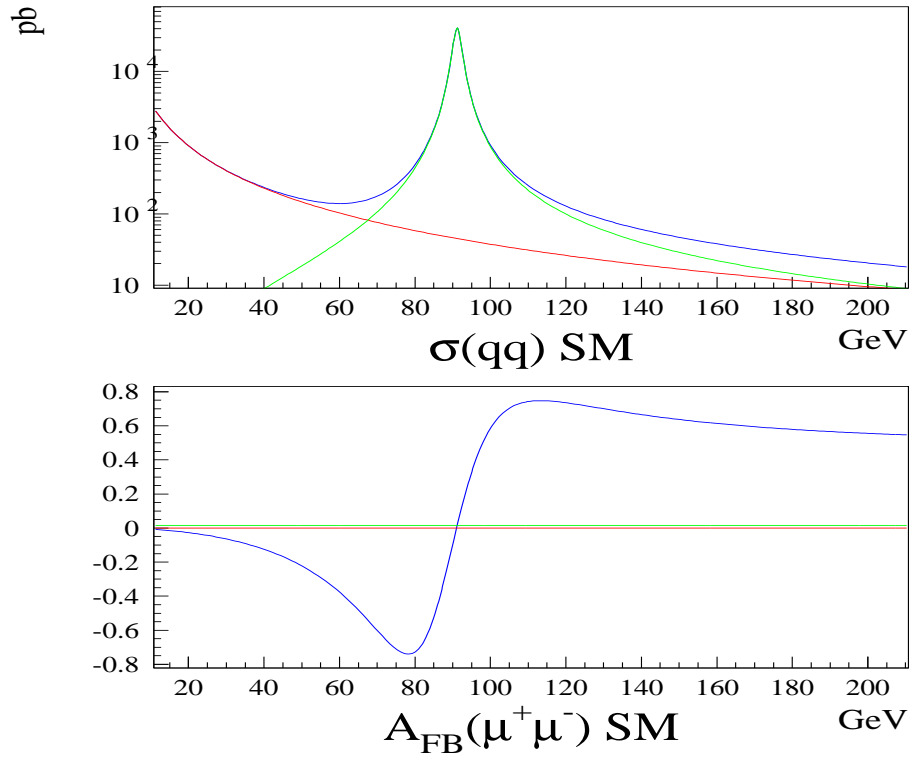


Figure 2: *Hadron cross section and muon forward-backward asymmetry in e^+e^- collisions (red - photon exchange, green - Z exchange, blue - total).*

The interest in studying fermion-pair final states at LEP2 is driven by the fact that many types of new physics scenarios can contribute to these processes, as shown by the last amplitude in Equation (1). For this to happen, the couplings to the initial and final states should be different from zero. In this case, even if the Standard Model extension operates at an energy scale much higher than the accessible centre-of-mass energy for a direct observation, it can still

give measurable effects by modifying the differential cross section through interference with the SM amplitudes.

Contact Interactions

Contact interactions offer a general framework for describing a new interaction with typical energy scale $\Lambda \gg \sqrt{s}$. The presence of operators with canonical dimension $N > 4$ in the Lagrangian gives rise to effects $\sim 1/M^{N-4}$. Such interactions can occur for instance, if the SM particles are composite, or when new heavy particles are exchanged.

For fermion- or photon-pair production the contact interactions are described by the diagrams shown in Figure 3. In the fermion case, the lowest order flavor-diagonal and helicity-conserving operators have dimension six [1]. For photons the lowest order operators have dimension eight, leading to suppression of the interference terms as the inverse forth power of the relevant energy scale.

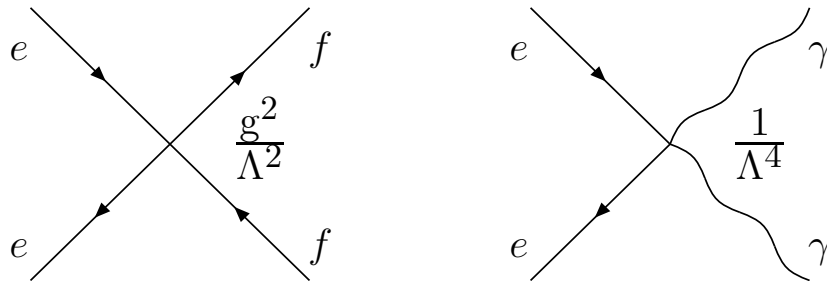


Figure 3: *Contact interaction diagrams for difermion or diphoton final states.*

The differential cross section takes the form

$$\frac{d\sigma}{d\Omega} = SM(s, t) + \varepsilon \cdot C_{Int}(s, t) + \varepsilon^2 \cdot C_{NewPh}(s, t) \quad (2)$$

where the first term is the Standard Model contribution, the second comes from interference between the SM and the contact interaction, and the third is the pure contact interaction effect. The Mandelstam variables are denoted as s , t and u .

Usually the coupling is fixed, and the structure of the interaction is parametrized by coefficients for the helicity amplitudes:

$$\begin{array}{ll} g & \text{coupling (by convention } \frac{g^2}{4\pi} = 1) \\ |\eta_{ij}| \leq 1 & \text{helicity amplitudes } (i, j = \text{L, R}) \\ \varepsilon & \frac{g^2 \text{sign}(\eta)}{4\pi \Lambda^2} \text{ for } f\bar{f}; \quad \sim \frac{1}{\Lambda^4} \text{ for } \gamma\gamma \end{array}$$

Some often investigated models are summarized in Table 2. The models in the second half of the table are parity conserving, and hence not constrained by the very precise measurements of atomic parity violation at low energies. The results presented in this contribution cover the models in the table and, as we will see in a moment, have connection to the recent searches for extra spatial dimensions.

As an illustration the effects of contact interactions for one particular model are shown in Figure 4.

Table 2: Contact interaction models.

Model	LL	RR	LR	RL	VV	AA	LL+RR	LR+RL
	Non-parity conserving				Parity conserving			
η_{LL}	± 1	0	0	0	± 1	± 1	± 1	0
η_{RR}	0	± 1	0	0	± 1	± 1	± 1	0
η_{LR}	0	0	± 1	0	± 1	∓ 1	0	± 1
η_{RL}	0	0	0	± 1	± 1	∓ 1	0	± 1

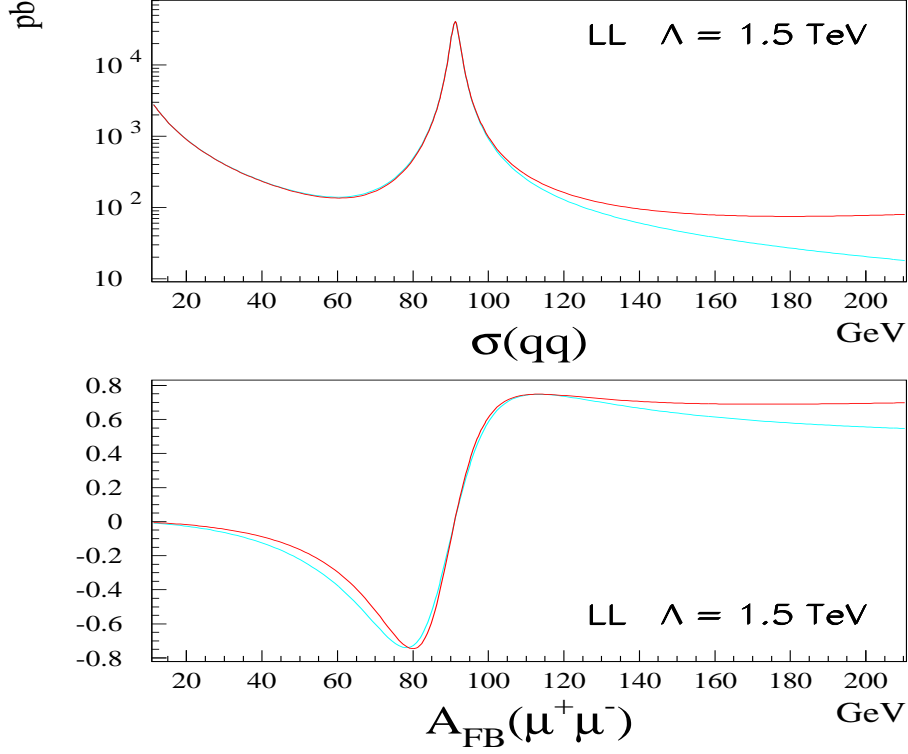


Figure 4: *Hadron cross section and muon forward-backward asymmetry in e^+e^- collisions in the presence of contact interactions (cyan - Standard Model, red - with contact interactions).*

Low Scale Gravity

The fastest progress in physics comes when we deepen our understanding of space-time. The development of string theory points to the existence of up to seven additional dimensions, which are compactified at very small distances, initially estimated to be $\sim 10^{-32}$ m, and hence far below the scales probed at high energy colliders. Recently, a radical proposal [2] has been put forward for the solution of the hierarchy problem, which brings close the electroweak scale $m_{EW} \sim 1$ TeV and the Planck scale $M_{Pl} \sim \frac{1}{\sqrt{G_N}} \sim 10^{15}$ TeV. In this framework the effective four-dimensional M_{Pl} is connected to a new $M_{Pl(4+n)}$ scale in a $(4+n)$ dimensional theory:

$$M_{Pl}^2 \sim M_{Pl(4+n)}^{2+n} R^n \quad (3)$$

where there are n extra compact spatial dimensions of radius $\sim R$, which could be as large as 1 mm. This can explain the observed weakness of gravity at large distances. At the same time,

quantum gravity becomes strong at a scale M of the order of few TeV and could have observable signatures at present and future colliders. The attractiveness of this proposal is enhanced by the plethora of expected phenomenological consequences described by just a few parameters.

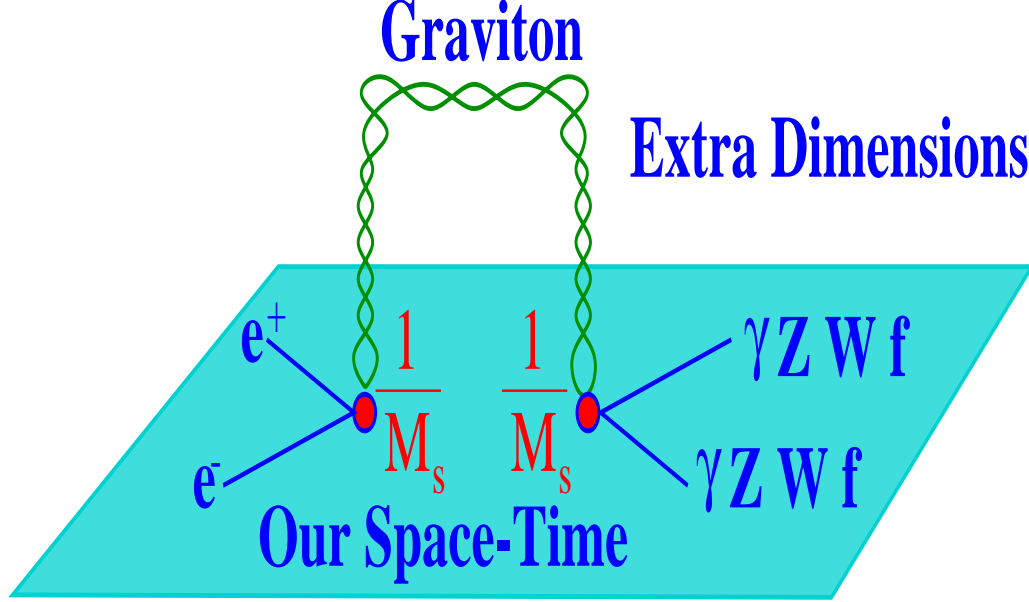


Figure 5: *Virtual graviton exchange diagrams for difermion or diboson final states.*

In the production of fermion- or boson-pairs in e^+e^- collisions this class of models can be manifested through virtual effects due to the exchange of gravitons (Kaluza-Klein excitations), depicted in Figure 5. As discussed in [5–8], the exchange of spin-2 gravitons modifies in a unique way the differential cross sections for fermion pairs, providing clear signatures. These models introduce an effective scale (cut-off), denoted as M_s in [5,6], as Λ_T in [7] and again as M_s in [8]. The first two scales are connected by the relation $M_s = (2/\pi)^{1/4}\Lambda_T$, which gives numerically $\Lambda_T = 1.1195 M_s$. They do not depend on the number of extra dimensions. In the third case the scale exhibits such a dependence; the relation to the other scales is given by $M_s^{HLZ}|_{n=4} = \Lambda_T$ for four extra dimensions. As the majority of LEP experiments has decided to use the scale M_s of [5], we will stick to this notation throughout this paper, and convert the experimental results when necessary to facilitate the comparison. The cut-off scale is supposed to be of the order of the fundamental gravity scale M in $4+n$ dimensions. The results are model-dependent, which is usually expressed by the introduction of an additional parameter

$$\frac{\lambda}{M_s^4}. \quad (4)$$

The value of λ is not known exactly, the usual assumption is $\lambda = \pm 1$ to allow for both constructive and destructive interference effects.

String Models

The ideas outlined in the previous subsection have triggered new developments, which propose concrete string realizations of the large extra dimensions scenario. We will discuss two models of this type.

As noted in [9], the low-energy effective theory that we are dealing with is derived from an underlying theory of quantum gravity. And the only known consistent framework for the

description of quantum gravity is superstring theory. In string models the SM particles are extended structures, represented by massless modes of open strings on a set of branes. In this model massive string mode oscillations (called *TeV strings*) give rise to dimension-8 operators which modify the SM amplitudes and are expected to dominate over the effects coming from Kaluza-Klein excitations. The model has two basic parameters: the dimensionless Yang-Mills coupling constant g_{YM} and the string scale - M_S ¹. The relation to the fundamental gravitational scale M is depending on the coupling

$$\frac{M}{M_S} = \left(\frac{1}{\pi}\right)^{1/8} \alpha^{-1/4}; \quad LSG \text{ scale } M \sim 1.6 - 3.0 M_S \quad (5)$$

where $\alpha = g_{YM}^2/4\pi$, and the values 3.0 (1.6) correspond to $\alpha = 1/137$ ($\alpha_s(1 \text{ TeV})$) respectively.

In this model the tree-level open string four-point amplitudes are multiplied by a string form factor (first introduced by G. Veneziano [11])

$$\mathcal{S}(s, t) = \frac{\Gamma(1 - \frac{s}{M_S^2})\Gamma(1 - \frac{t}{M_S^2})}{\Gamma(1 - \frac{s}{M_S^2} - \frac{t}{M_S^2})}. \quad (6)$$

For $e^+e^- \rightarrow e^+e^-$ the differential cross section is modified:

$$\frac{d\sigma}{d\cos\theta} = \left(\frac{d\sigma}{d\cos\theta}\right)_{SM} \cdot |\mathcal{S}(s, t)|^2. \quad (7)$$

For $e^+e^- \rightarrow \gamma\gamma$ one can use Drell's parametrization (QED cut-off, *cf.* next subsection)

$$\Lambda_+^{QED} = \left(\frac{12}{\pi^2}\right)^{1/4} \cdot M_S = 1.05 M_S. \quad (8)$$

In a new *D-brane model* [12], the Standard Model matter fields are identified with massless modes of open strings stretched between two sets of branes - D3 and D7 branes (37 strings). In this scenario we can have dimension-6 operators due to contact interactions induced by massive string oscillators. These effects can be stronger than the ones coming from Kaluza-Klein states or winding modes and will dominate the dimension-8 operators coming from TeV strings.

Photon-pair Production

The production of photon pairs in e^+e^- collisions is described by the t - and u -channel QED diagrams depicted in Figure 6.

The differential cross section has the following simple form

$$\frac{d\sigma}{d\Omega} = |e_t + e_u + \text{New Physics ?!}|^2 \quad (9)$$

$$\left(\frac{d\sigma}{d\Omega}\right)_{QED} = \frac{\alpha^2}{2s} \left[\frac{t}{u} + \frac{u}{t}\right] = \frac{\alpha^2}{s} \cdot \frac{1 + \cos^2\theta}{1 - \cos^2\theta}. \quad (10)$$

The experiments have investigated many proposed deviations from QED:

¹ The effective gravity cut-off scale with subscript small s from the previous subsection should not be confused with the string scale M_S , studied here.

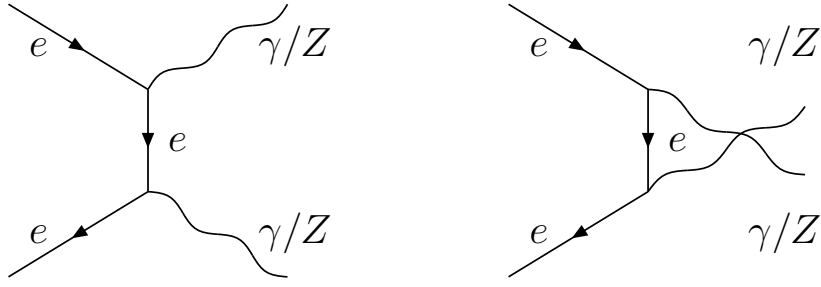


Figure 6: *Feynman diagrams for diphoton (di-Z) final states.*

$$\frac{d\sigma}{d\Omega} = \left(\frac{d\sigma}{d\Omega} \right)_{QED} \cdot \left(1 \pm \frac{1}{(\Lambda_{\pm}^{QED})^4} \cdot \frac{s^2}{2} \sin^2 \theta \right) \quad (11)$$

$$\frac{d\sigma}{d\Omega} = \left(\frac{d\sigma}{d\Omega} \right)_{QED} \cdot \left(1 \mp \frac{\lambda}{\pi\alpha(M_s)^4} \cdot \frac{s^2}{2} \sin^2 \theta + \dots \right) \quad (12)$$

$$\frac{d\sigma}{d\Omega} = \left(\frac{d\sigma}{d\Omega} \right)_{QED} \cdot \left(1 + \frac{\pi^2}{12(M_S)^4} \cdot \frac{s^2}{2} \sin^2 \theta \right) \quad (13)$$

$$\frac{d\sigma}{d\Omega} = \left(\frac{d\sigma}{d\Omega} \right)_{QED} \cdot \left(1 + \frac{(\eta_L + \eta_R)}{2(\Lambda^{CI})^4} \cdot \frac{s^2}{2} \sin^2 \theta + \dots \right) \quad (14)$$

$$\frac{d\sigma}{d\Omega} = \left(\frac{d\sigma}{d\Omega} \right)_{QED} \cdot \left(1 + \frac{2}{\alpha(\Lambda_6)^4} \cdot \frac{s^2}{2} \sin^2 \theta + \dots \right) \quad (15)$$

$$\frac{d\sigma}{d\Omega} = \left(\frac{d\sigma}{d\Omega} \right)_{QED} \cdot \left(1 + \frac{s^3}{32\pi\alpha^2(\Lambda')^6} \frac{\sin^2 \theta}{1 + \cos^2 \theta} + \dots \right). \quad (16)$$

The QED cut-off - Equation (11), is the basic form of possible deviations from quantum electrodynamics. If we ignore higher order terms (given by ...), all equations except Equation (16) predict the same form of deviations in the differential cross section. Equation (12) is the low scale gravity case [7, 14], and Equation (13) appears in the TeV strings model. The others are variations of contact interactions. I have chosen to compile the deviations in a similar form, which makes it particularly easy to compare the results from different searches by transforming the relevant parameters.

2 Fermion-pair production: $e^+e^- \rightarrow f\bar{f}(\gamma)$

$f\bar{f}$ - Signal Definition

The large data samples accumulated at LEP2 have propelled the measurements of several final states in the precision area, where many tiny theoretical details or experimental systematic effects start to grow in importance. For instance, the signal definition for fermion pairs is complicated by several factors:

- Interplay between two-fermion and four-fermion final states: the radiative corrections include not only effects due to vector bosons, but also contributions from real and virtual fermion pairs, *cf.* Figure 7. For example, low mass (secondary) fermion pairs are part of the signal, like photons. The situation is ambiguous if the two final state fermion

pairs carry the same flavor or roughly the same energy. Fortunately these corrections are negligible for the non-radiative (genuine high energy) sample, which is the main search field for physics beyond the SM ².

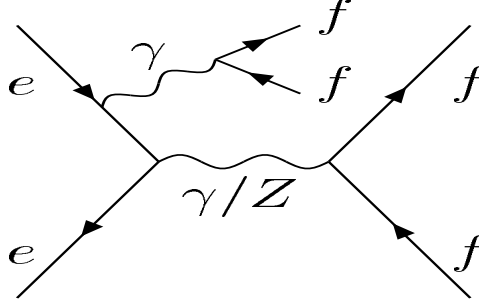


Figure 7: One example of Feynman graph contributing to pair-corrections in fermion-pair production.

- The definition of the effective (propagator in Figure 1) energy s' is not unique due to interference between initial- and final-state radiation:
 - the interference changes the cross-sections: for $\sqrt{s'}/\sqrt{s} > 0.85$ by $\sim 1.5\%$ for $\mu^+\mu^-$ and $\sim 0.5\%$ for $q\bar{q}$ in order $\mathcal{O}(\alpha)$ (the experimental efficiency is changed by $\leq 50\%$ of this)
 - the experiments either apply a correction by subtracting the interference contribution, rendering the $\sqrt{s'}$ definition unique, or define $\sqrt{s'}$ as the effective mass of the outgoing fermion pair after final state radiation; there is no unanimity about the “best” definition, requiring the minimal amount of theoretical corrections; for a detailed discussion we refer the reader to [16].
- Rising four-fermion background: LEP2 is the kingdom of double (or single) weak boson production like W^+W^- , ZZ , $Z e^+e^-$, $W e\nu$, ...

Fermion Pairs - Selection

The event selection for the different final states is illustrated on Figure 8. For e^+e^- it is ‘quite easy’, and consists of requiring an identified electron-positron pair (typically tracks matched to electromagnetic energy deposits). The huge peak at electron (or positron) energy in the vicinity of the beam energy is due to the large contribution from t -channel photon exchange. The backgrounds are tiny. For $q\bar{q}$ the selection is ‘easy’, and asks for high multiplicity relatively balanced events with substantial visible energy. The high energy peak is accompanied by a huge peak due to radiative ‘Z returns’, favored by the large hadron cross section at the Z pole. For $\mu^+\mu^-$ the selection is ‘still easy’, asking for two muons identified as tracks in the muon chambers or as minimum ionizing objects in the calorimeters. The ratio of the muon and beam momenta clearly separates the signal from various backgrounds peaking at low energies. Cosmic muons complicate the picture, and are typically suppressed by imposing space-time constraints on the tracks to originate from beam interactions.

²For an early review of searches above the Z pole see *e.g.* [15].

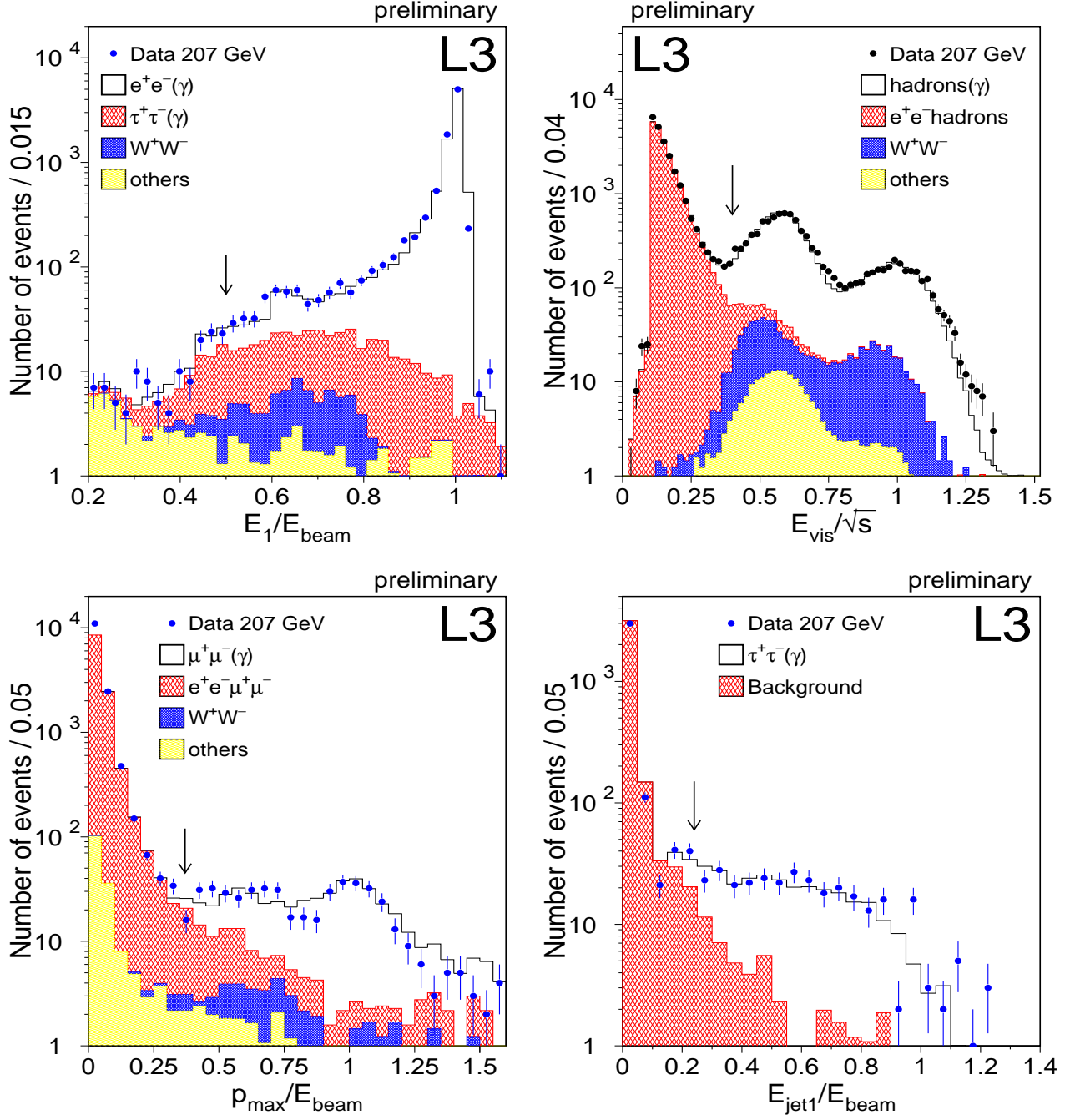


Figure 8: Typical plots for the event selection of the various final states (e^+e^- , $q\bar{q}$, $\mu^+\mu^-$, $\tau^+\tau^-$) in the L3 experiment.

For $\tau^+\tau^-$ the selection is ‘far from easy’, and consists typically of requiring two narrow low multiplicity jets. The ratio of jet to beam energy suppresses low energy backgrounds, and the peak at one is absent due to the neutrinos from τ decays. Bhabha backgrounds are dangerous, especially if there are problems with energy measurements in the endcaps.

LEP2 $f\bar{f}$ Group

Following the LEP tradition, a Fermion-pair Subgroup of the LEP Electroweak Working Group has been established in 1999 in order to combine the measurements of total and differential cross sections σ_{tot} and $\frac{d\sigma}{d\cos\theta}$, of forward-backward asymmetries A_{FB} , and of the ratios of heavy flavor to total hadronic cross sections for beauty and charmed quarks R_b and R_c . In this way the statistical error of the combined measurements is reduced by a factor of two, and several types of correlated systematic errors, *e.g.* in one experiment between different centre-of-mass energies or between all experiments, can be properly taken into account. The group also provides a very useful forum for exchange of ideas and facilitates the convergence of the signal definitions used by the different collaborations, making the task of combining the measurements much easier.

At the moment of this writing we have succeeded to combine the published results [17, 18, 20, 29] and preliminary measurements [32, 35, 37, 39] for the following final states: $\mu^+\mu^-$, $\tau^+\tau^-$, $q\bar{q}$, $b\bar{b}$ and $c\bar{c}$. The results [41] are shown in the next subsection. They are used to perform combined fits searching for contact interactions or for Z' .

The future plans of the group include combining the measurements of the e^+e^- and $\gamma\gamma$ final states. In the absence of LEP-wide combined measurements, for the purpose of this talk I have followed a top-down approach and extracted limits on models beyond the Standard Model by fitting directly the preliminary results of the four LEP collaborations for e^+e^- , or by using as input the results of the fits for the QED cut-off of the individual experiments for $\gamma\gamma$.

Results

The combined results for the total cross section σ_{tot} and for the forward-backward asymmetry A_{FB} are shown in Figure 9. In the same figure the measurements for b and c quarks are shown. They agree well with the SM expectations above the Z resonance. A special case is the hadron cross section, which shows the tendency to lie above the SM line, computed with ZFITTER [42]. The averaged cross section is between 2 and 3 standard deviations away from the expectation, depending on the assigned normalization uncertainty. The high precision of the measurements requires improvements in the theoretical uncertainty and independent cross-checks.

3 Photon-pair production: $e^+e^- \rightarrow \gamma\gamma(\gamma)$

The event selection is similar to the one for e^+e^- , with the major difference that here the (absence of) tracking information is used to veto tracks associated with the electromagnetic clusters, and there is no need to recognize the electric charge. Measurements of total and differential cross sections for $\gamma\gamma$ final states [43] are shown in Figure 10. The results include the 2000 data up to 209 GeV (for ALEPH they are up to 202 GeV). Good agreement with the SM expectations is observed.

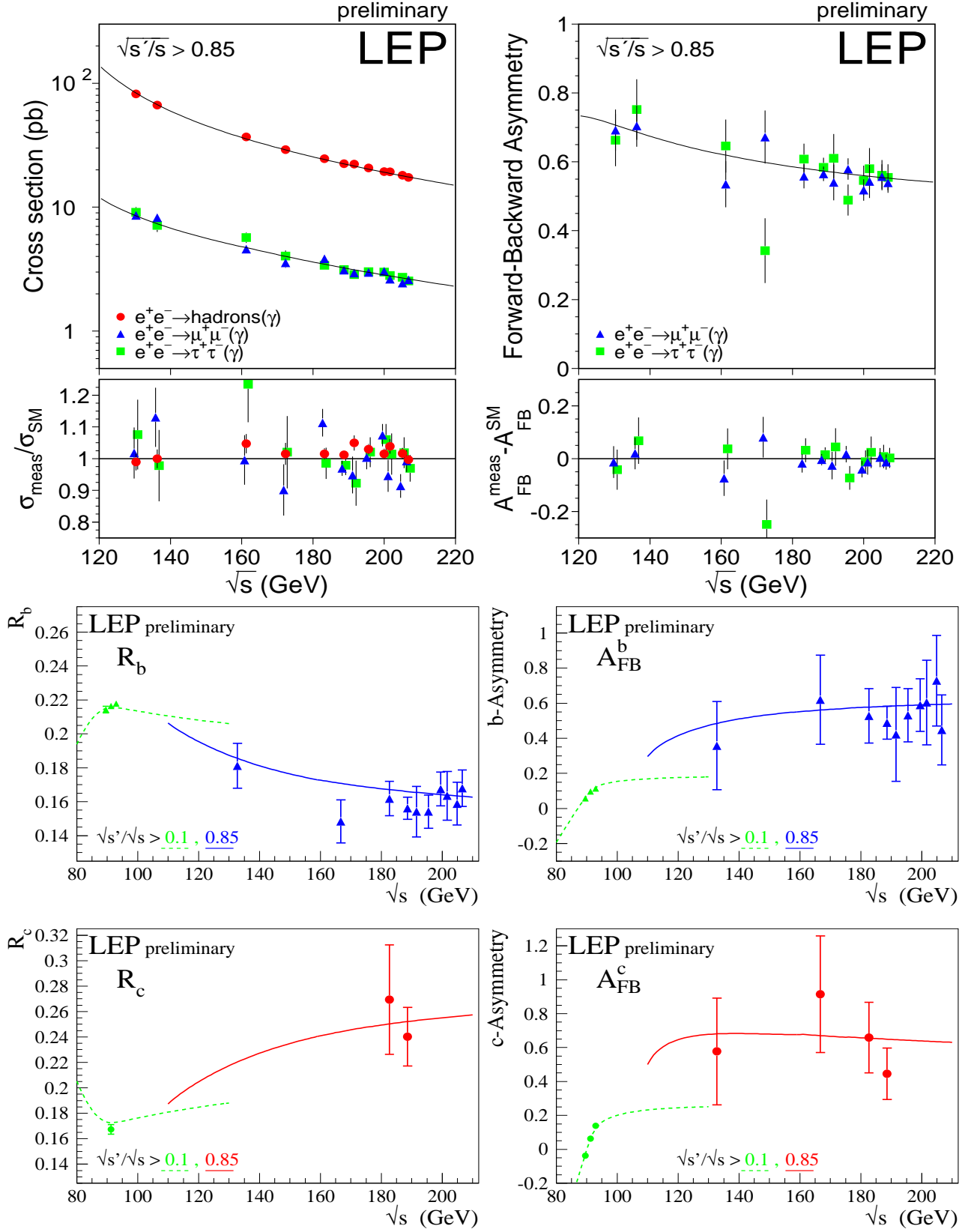


Figure 9: Total cross sections and forward-backward asymmetries for $\mu^+\mu^-$, $\tau^+\tau^-$ and $q\bar{q}$ (upper half). R_b and A_{FB}^b for b (middle), R_c and A_{FB}^c for c (lower quarter) quarks.

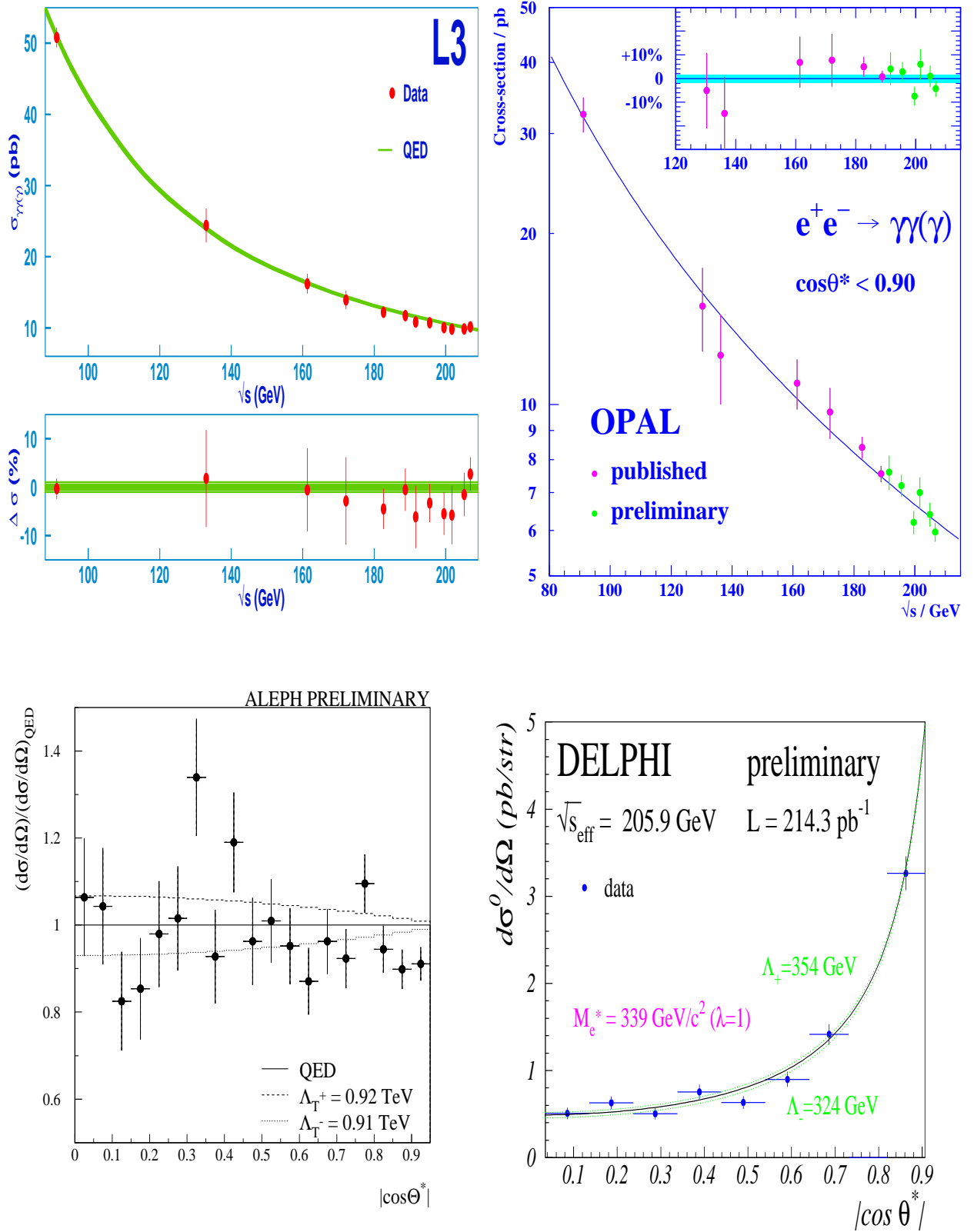


Figure 10: Total cross section measurements for diphoton final states from L3 and OPAL. Ratio of the differential cross section to the SM from ALEPH and the effects expected in low scale gravity models. Differential cross section measurements from DELPHI and the fit results for QED cut-offs and excited electrons.

4 Searches for New Phenomena: Contact Interactions and Extra Dimensions

The LEP measurements show no statistically significant deviations from the SM predictions. In their absence we present limits at 95 % confidence level on several new physics proposals. The LEP2 $f\bar{f}$ group has derived limits on contact interactions [41] for $\mu^+\mu^-$, $\tau^+\tau^-$ and the two channels combined (Table 3, Figure 11a), for $q\bar{q}$, $b\bar{b}$ (Figure 11b) and $c\bar{c}$.

Table 3: Limits on contact interactions at 95% CL.

$e^+e^- \rightarrow \mu^+\mu^-$				$e^+e^- \rightarrow \tau^+\tau^-$		
Model	ε [TeV ⁻²]	Λ^- [TeV]	Λ^+ [TeV]	ε [TeV ⁻²]	Λ^- [TeV]	Λ^+ [TeV]
LL	$-0.0056^{+0.0040}_{-0.0040}$	8.6	14.7	$-0.0016^{+0.0054}_{-0.0047}$	9.4	10.6
RR	$-0.0077^{+0.0053}_{-0.0030}$	8.3	14.1	$-0.0008^{+0.0049}_{-0.0060}$	9.0	10.2
VV	$-0.0014^{+0.0016}_{-0.0017}$	15.3	22.4	$-0.0002^{+0.0016}_{-0.0023}$	15.2	17.5
AA	$-0.0036^{+0.0027}_{-0.0013}$	11.8	20.4	$-0.0004^{+0.0032}_{-0.0025}$	13.2	13.8
LR	$0.0014^{+0.0043}_{-0.0061}$	7.8	9.3	$-0.0014^{+0.0075}_{-0.2283}$	2.1	8.6
RL	$0.0014^{+0.0043}_{-0.0061}$	7.8	9.3	$-0.0014^{+0.0075}_{-0.2283}$	2.1	8.6
V0	$-0.0036^{+0.0025}_{-0.0014}$	12.1	20.2	$-0.0003^{+0.0023}_{-0.0030}$	13.0	14.7
A0	$0.0008^{+0.0020}_{-0.0031}$	12.7	12.9	$-0.0008^{+0.0038}_{-0.0046}$	9.9	11.9

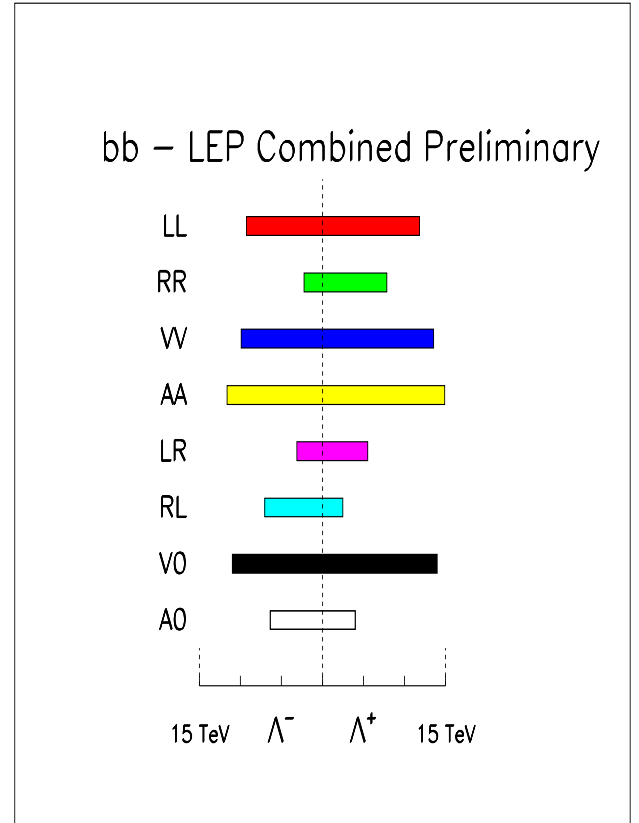
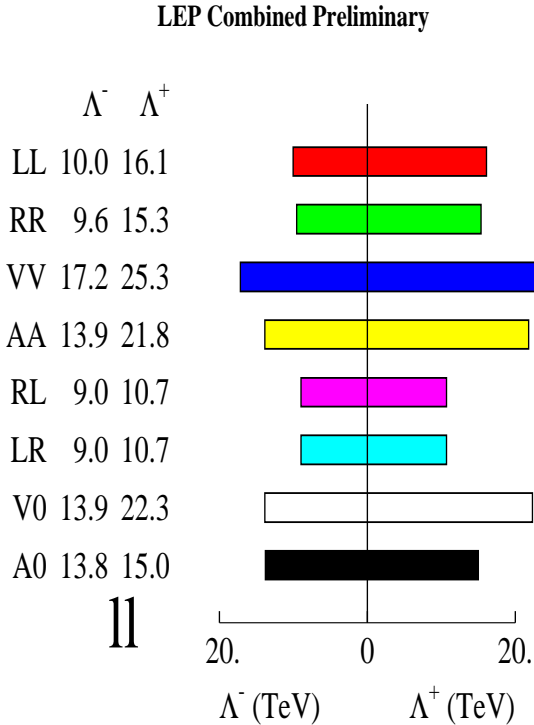


Figure 11: Limits on contact interactions at 95% CL. a - for $\mu^+\mu^-$ and $\tau^+\tau^-$ combined (ll), b - for $b\bar{b}$.

For many models the limits are in the 10–20 TeV range. It is interesting to compare them with the expectations back in 1988 [47]. The actual limits are typically a factor two better, mainly due to the successful running of LEP above the anticipated maximum energy of 190 GeV. Another factor is the combination of the results from the four collaborations.

The values for ε from Table 3 are maximally 1.5 standard deviations away from the Standard Model value $\varepsilon = 0$. The recent measurement from the E821 experiment at BNL [48] on the anomalous magnetic moment of the muon shows a 2.6 standard deviations discrepancy with theory. As pointed out in [49], if the experimental result is ascribed to muon substructure, the model-independent limit on the energy scale is $1.2 \text{ TeV} < \Lambda_\mu < 3.2 \text{ TeV}$ at 95 % CL. The LEP limits from $e^+e^- \rightarrow \mu^+\mu^-$ are based on the assumption of a common energy scale for electrons and muons: $\Lambda_e \simeq \Lambda_\mu$. While there is no *a priori* reason for the first- and second-generation lepton substructure scales to be close, the 10–20 TeV range of the LEP limits implies a very high scale for electrons if the new experimental result is originating from muon compositeness.

Some experiments [50] have updated their limits on the low gravity or TeV string scales, using the most sensitive channel at LEP2 - Bhabha scattering [52, 53]. The measurements are compared to the SM or to theories with large extra dimensions in Figure 12. The results are:

$$\text{L3} : M_s^+ > 1.06 \text{ TeV} \quad M_s^- > 0.98 \text{ TeV} \quad \text{TeV Strings} : M_s > 0.57 \text{ TeV} \quad (17)$$

$$\text{OPAL} : M_s^+ > 1.00 \text{ TeV} \quad M_s^- > 1.15 \text{ TeV}. \quad (18)$$

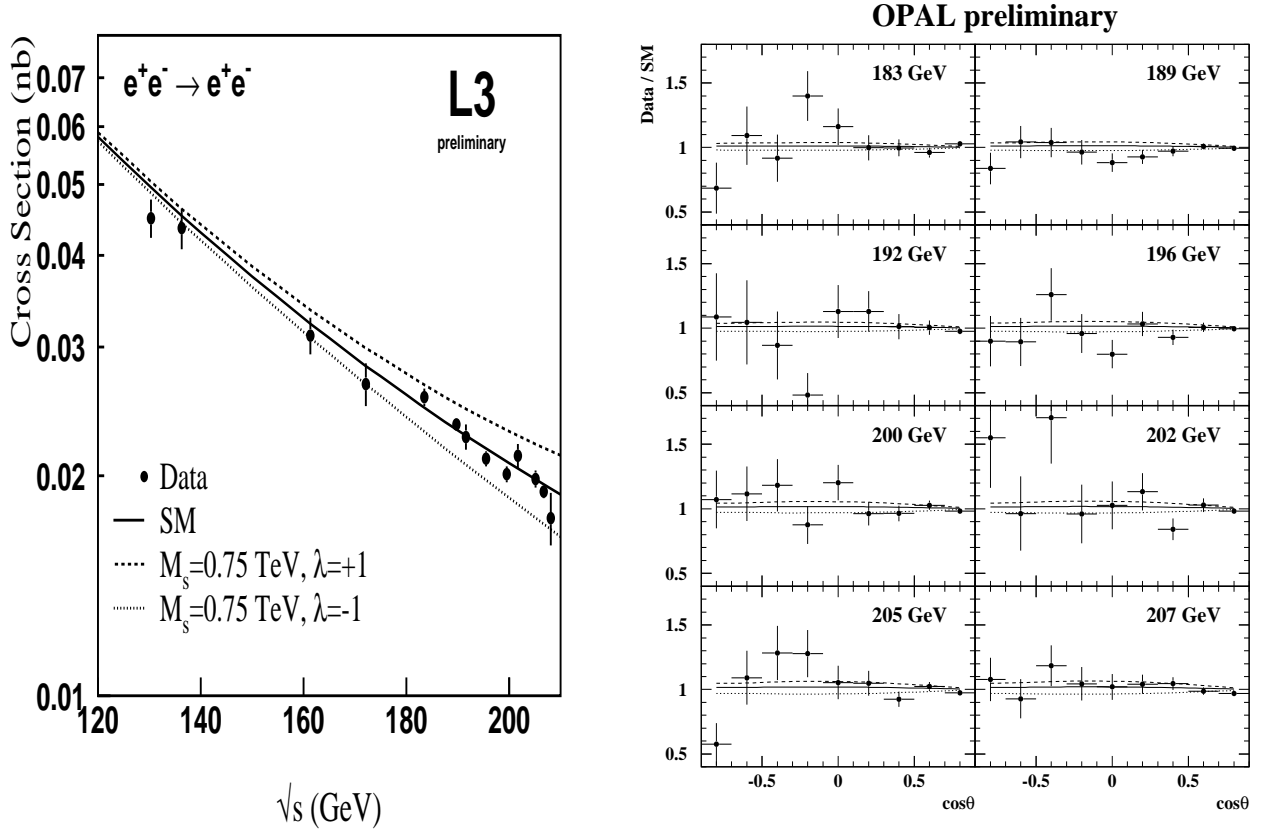


Figure 12: Measurements of the reaction $e^+e^- \rightarrow e^+e^-$ and searches for low scale gravity effects: left - total cross sections from L3, right - differential cross sections from OPAL.

The reaction $e^+e^- \rightarrow \gamma\gamma$ is a sensitive “QED laboratory”. The limits obtained by the LEP experiments [43] are compiled in Table 4. In the last column of the table I have combined the limits, using as input the results of the fits for the QED cut-off of the individual collaborations. Here the assumption that the log-likelihood curve in the variable $1/\Lambda^4$ can be approximated with one coming from the normal distribution is made. Then it is straightforward to combine the measurements and to extract LEP-wide limits. The individual results are very close to this behaviour, and the resulting uncertainty in the limits is only a few %. This is used further as input to translate the limits in the language of low scale gravity and TeV strings, taking into account also the sign conventions.

Table 4: Limits on new physics from $\gamma\gamma$ at 95 % CL.

Mo- del	ALEPH [TeV]	DELPHI [TeV]	L3 [TeV]	OPAL [TeV]	Combined (DB) [TeV]
QED cut-off - Λ_{\pm}^{QED}					
Λ_+	0.319	0.354	0.385	0.344	0.44
Λ_-	0.317	0.324	0.325	0.325	0.37
excited electron: $m_{e^*}^2/\lambda \sim (\Lambda^{QED})^2$					
M_{e^*}	0.337	0.339	0.325	0.354	-
low scale gravity: $M_s^{\pm} = 2.57 \Lambda_{\mp}^{QED}$; $\Lambda_T = 1.1195 M_s$					
M_s^+	0.81	0.83	0.83	0.83	0.95
M_s^-	0.82	0.91	0.99	0.89	1.14
TeV strings: $M_S = 0.952 \Lambda^{QED}$					
M_S	0.304	0.337	0.367	0.327	0.42
contact interactions: $\Lambda_6 = 4.069 \Lambda^{QED}$					
Λ_6	1.299		1.566		
more contact interactions: Λ'					
Λ'			0.810	0.763	

The need to obtain combined limits on the low gravity scale has been recognized early [52, 54, 56], and LEP results are shown in Table 5, together with the new L3 and OPAL limits presented for this conference. In the last part of the table the results of combined fits to the preliminary measurements of σ_{tot} and A_{FB} for Bhabha scattering are shown. Here I have updated the analysis [52], applying the same technique. The highest energy LEP data on e^+e^- and $\gamma\gamma$ clearly improve the sensitivity of the first combined analyses, which used data up to 189 GeV. Applying the method for combining the $\gamma\gamma$ limits, described above, a LEP-wide limit, shown in the last row of Table 5, is extracted from the two most sensitive channels.

It is interesting to compare the newest LEP limits with the results from other colliders. The DØ collaboration at FNAL has performed an analysis [57] using events containing a pair of electrons or photons, which turn out to give the highest sensitivity at the TEVATRON. The two-dimensional distribution in invariant mass and polar angle is fitted. The result is:

$$D\emptyset : M_s^+ > 1.1 \text{ TeV} \quad M_s^- > 1.0 \text{ TeV}. \quad (19)$$

It is interesting to note that in spite of the low statistics at high mass, the extended energy coverage of the hadron collider is helpful, and the limits are pretty close to the most stringent

lower limits to date, coming from LEP - *cf.* Table 5. Run II at the TEVATRON can improve substantially the results [58], especially by accumulating events at high mass.

The H1 collaboration has presented limits [59] from deep inelastic scattering at HERA:

$$\text{H1 : } M_s^+ > 0.43 \text{ TeV} \quad M_s^- > 0.64 \text{ TeV}. \quad (20)$$

These limits are somewhat lower than those from LEP or the TEVATRON, and the next run is expected to improve the sensitivity.

Table 5: Limits on low scale gravity at 95 % CL.

Process	LSG scale M_s (TeV)	
	$\lambda = -1$	$\lambda = +1$
D.Bourilkov, JHEP 08 (1999) 006; hep-ph/9907380		
$e^+e^- \rightarrow e^+e^-$ (LEP combined < 189 GeV)	0.96	1.26
S.Mele, E.Sanchez, PRD 61(2000)117901; hep-ph/9909294		
$e^+e^- \rightarrow \text{bosons}$ (LEP combined < 189 GeV)	0.96	0.93
Winter Conf. 2001 - preliminary		
$e^+e^- \rightarrow e^+e^-$ (L3)	0.98	1.06
$e^+e^- \rightarrow e^+e^-$ (OPAL)	1.15	1.00
Winter Conf. 2001 - LEP combined preliminary (DB)		
$e^+e^- \rightarrow e^+e^-$	1.28	1.13
$e^+e^- \rightarrow \gamma\gamma$	1.14	0.95
$e^+e^- \rightarrow e^+e^-$ and $e^+e^- \rightarrow \gamma\gamma$	1.39	1.13

The L3 collaboration has updated the limit on the TeV strings scale, as shown in Table 6. In this table also the combined limit extracted from the latest results for the $\gamma\gamma$ final state is shown. The limits are still below the result from the first combined analysis [53].

Table 6: Limits on TeV strings at 95 % CL.

Process	TeV strings scale M_S (TeV)
D.Bourilkov, PRD 62(2000)076005; hep-ph/0002172	
$e^+e^- \rightarrow e^+e^-$ (LEP combined < 189 GeV)	0.63
Winter Conf. 2001 - preliminary	
$e^+e^- \rightarrow e^+e^-$ (L3)	0.57
$e^+e^- \rightarrow \gamma\gamma$ (LEP combined - DB)	0.42

The last model investigated here is contact interaction coming from two sets of D-branes [12]. In the case of muons and taus we can use directly the limits obtained by the LEP2 $f\bar{f}$ group for the VV model with positive interference. The scales are connected as:

$$e^+e^- \rightarrow \mu^+\mu^-, \tau^+\tau^- : \eta_{LL} = \eta_{RR} = \eta_{LR} = \eta_{RL} = 1 \quad (21)$$

$$\Lambda_{VV}^+ \simeq \sqrt{\frac{4\pi}{0.59g_S}} \cdot M_S. \quad (22)$$

The value of the coupling constant g_S is not known exactly, and the results are given for $g_S = g_{YM}^2 \sim \frac{1}{2}$, with g_{YM} the gauge coupling, and for the extreme choice $\frac{g_S}{4\pi} = \frac{1}{128}$.

For electrons the D-brane model predicts a novel type of helicity structure:

$$e^+e^- \rightarrow e^+e^- : 0.75\eta_{LL} = 0.75\eta_{RR} \simeq \eta_{LR} = \eta_{RL} = 1 \quad (23)$$

so we can not use directly limits provided by the individual experiments. A dedicated analysis is performed, using as input the preliminary measurements of σ_{tot} and A_{FB} for Bhabha scattering from the four LEP collaborations. The results are summarized in Table 7. They show a significant improvement compared to the limits in [12], due to the inclusion of the electron channel and the 2000 data.

Table 7: Limits on contact interactions in D-brane models at 95 % CL.

Process	D-brane string scale M_S (TeV)	
	$g_S = g_{YM}^2 \sim \frac{1}{2}$	$\frac{g_S}{4\pi} = \frac{1}{128}$
Winter Conf. 2001 - LEP combined preliminary (DB)		
$e^+e^- \rightarrow \mu^+\mu^-$ and $e^+e^- \rightarrow \tau^+\tau^-$	3.9	1.7
$e^+e^- \rightarrow e^+e^-$	3.5	1.5

5 Outlook

A short summary:

- ♣ the Standard Model has no difficulty to describe the full set of precise LEP2 measurements from 130-209 GeV (results at 192–209 GeV are preliminary)
- ◇ the extra dimensions remain hidden so far ...
in spite of sensitive searches!
- ♡ many new limits (some deep in the TeV scale!) for physics
beyond the Standard Model
- ♠ let us hope that some of the future speakers will be more lucky and will announce

LHC NEWS : STRING DISCOVERY?

Acknowledgements

The author is grateful to the four LEP collaborations for providing their latest results. Special thanks go to the members of the LEP2 $f\bar{f}$ group for the constructive work being done together. I would like to thank I. Antoniadis, K. Benakli, G. Giudice, S. Mele, M. Peskin and F. Schrempp for valuable discussions.

References

- [1] E. Eichten, K. Lane and M. Peskin, Phys. Rev. Lett. **50** (1983) 811
- [2] N.Arkani-Hamed, S. Dimopoulos and G. Dvali, Phys. Lett. **B 429** (1998) 263
- [3] I. Antoniadis, N. Arkani-Hamed, S. Dimopoulos and G. Dvali, Phys. Lett. **B 436** (1998) 257
- [4] N.Arkani-Hamed, S. Dimopoulos and G. Dvali, Phys. Rev. **D 59** (1999) 086004
- [5] J. Hewett, Phys. Rev. Lett **82** (1999) 4765
- [6] T. Rizzo, Phys. Rev. **D 59** (1999) 115010
- [7] G. Giudice, R. Rattazi and J. Wells, Nucl. Phys. **B 544** (1999) 3
- [8] T. Han, J.D. Lykken and R-J. Zhang, Phys. Rev. **D 59** (1999) 105006
- [9] E. Accomando, I. Antoniadis and K. Benakli, Nucl. Phys. **B 579** (2000) 3
- [10] S. Cullen, M. Perelstein and M. Peskin, Phys. Rev. **D 62** (2000) 055012
- [11] G. Veneziano, Nuovo Cim. **A 57** (1968) 190
- [12] I. Antoniadis, K. Benakli and A. Laugier, hep-th/0011281
- [13] I. Antoniadis, hep-th/0102202
- [14] K. Agashe, N.G. Deshpande, Phys. Lett. **B 456** (1999) 60
- [15] D. Bourilkov, LEP review talk, XXXIII Rencontres de Moriond, France, 1998; published in the proceedings ed. by J. Trân Thanh Vân, Edition Frontiers, Paris, 1999, page 139; hep-ex/9806027
- [16] Reports of the Working Groups on Precision Calculations for LEP2 physics; Two-fermion Production in Electron-positron Collisions, CERN-YR-2000-009, hep-ph/0007180
- [17] ALEPH Collaboration, R. Barate *et al.*, E. Phys. J. **C 12** (2000) 183
- [18] DELPHI Collaboration, P.Abreu *et al.*, Eur. Phys. J. **C 11** (1999) 383
- [19] DELPHI Collaboration, P.Abreu *et al.*, Phys. Lett. **B 485** (2000) 45
- [20] L3 Collaboration, M. Acciarri *et al.*, Phys. Lett. **B 370** (1996) 195
- [21] L3 Collaboration, M. Acciarri *et al.*, Phys. Lett. **B 407** (1997) 361

- [22] L3 Collaboration, M. Acciarri *et al.*, Phys. Lett. **B 479** (2000) 101
- [23] L3 Collaboration, M. Acciarri *et al.*, Phys. Lett. **B 485** (2000) 71
- [24] L3 Collaboration, M. Acciarri *et al.*, Phys. Lett. **B 414** (1997) 373
- [25] L3 Collaboration, M. Acciarri *et al.*, Phys. Lett. **B 433** (1998) 163
- [26] L3 Collaboration, M. Acciarri *et al.*, Phys. Lett. **B 464** (1999) 135
- [27] L3 Collaboration, M. Acciarri *et al.*, Phys. Lett. **B 470** (1999) 281
- [28] L3 Collaboration, M. Acciarri *et al.*, Phys. Lett. **B 489** (2000) 81
- [29] OPAL Collaboration, G. Abbiendi *et al.*, Eur. Phys. J. **C 2** (1998) 441
- [30] OPAL Collaboration, G. Abbiendi *et al.*, Eur. Phys. J. **C 6** (1999) 1
- [31] OPAL Collaboration, G. Abbiendi *et al.*, Eur. Phys. J. **C 13** (2000) 553
- [32] ALEPH Collaboration, ALEPH 99-018 CONF 99-013, CERN, 1999
- [33] ALEPH Collaboration, ALEPH 2000-047 CONF 2000-030, CERN, 2000
- [34] ALEPH Collaboration, ALEPH 2001-019 CONF 2001-016, CERN, 2001
- [35] DELPHI Collaboration, DELPHI 2000-128 OSAKA CONF 427, CERN, 2000
- [36] DELPHI Collaboration, DELPHI 2001-022 CONF 463, CERN, 2001
- [37] L3 Collaboration, L3 Note 2563, CERN, 2000
- [38] L3 Collaboration, L3 Note 2648, CERN, 2001
- [39] OPAL Collaboration, OPAL PN424, CERN, 2000
- [40] OPAL Collaboration, OPAL PN469, CERN, 2001
- [41] LEPEWWG $f\bar{f}$ Subgroup, Note LEP2FF/01-01 for Winter Conferences 2001, CERN, 2001; more details are given on the web page of the group: <http://lepewwg.web.cern.ch/LEPEWWG/lep2/>
- [42] ZFITTER version 6.21 is used.
D. Bardin *et al.*, e-print hep-ph/9908433; Zeit. f. Phys. **C 44** (1989) 493; Nucl. Phys. **B 351** (1991) 1; Phys. Lett. **B 255** (1991) 290
- [43] ALEPH Collaboration, ALEPH 2000-008 CONF 2000-005, CERN, 2000
- [44] DELPHI Collaboration, DELPHI 2001-023 CONF 464, CERN, 2001
- [45] L3 Collaboration, L3 Note 2650, CERN, 2001
- [46] OPAL Collaboration, OPAL PN469, CERN, 2001
- [47] B. Schrempp, F. Schrempp, N. Wermes and D. Zeppenfeld, Nucl. Phys. **B 296** (1988) 1
- [48] Muon g-2 Collaboration, H.N. Brown *et al.*, Phys. Rev. Lett. **86** (2001) 2227

- [49] K. Lane, hep-ph/0102131
- [50] L3 Collaboration, L3 Note 2647, CERN, 2001
- [51] OPAL Collaboration, OPAL PN471, CERN, 2001
- [52] D. Bourilkov, J. High Energy Phys. **08** (1999) 006 ; hep-ph/9907380
- [53] D. Bourilkov, Phys. Rev. **D 62** (2000) 076005; hep-ph/0002172
- [54] A. Gupta, N. Mondal and S. Raychaudhuri, report TIFR-HECR-99-02; hep-ph/9904234
- [55] K. Cheung, Phys. Lett. **B 460** (1999) 383
- [56] S. Mele and E. Sanchez, Phys. Rev. **D 61** (2000) 117901
- [57] DØ Collab., B. Abbott *et al.*, Phys. Rev. Lett. **86** (2001) 1156
- [58] K. Cheung and G. Landsberg, Phys. Rev. **D 62** (2000) 076003
- [59] H1 Collaboration, C. Adloff *et al.*, Phys. Lett. **B 479** (2000) 358.